

Study of Factors Influencing Dynamic Measurements Using SnO₂ Gas Sensor

Xingjiu Huang^{1*}, Fanli Meng, Yufeng Sun^{1,2} and Jinhuai Liu

Hefei Institute of Intelligent Machines, Chinese Academy of Sciences,
Hefei, 230031, P. R. China

¹Department of Chemistry, University of Science and Technology of China,
Hefei, 230026, P. R. China

²Department of Machines, Anhui University of Technology and Science,
Wuhu, 241000, P. R. China

(Received June 14, 2004; accepted November 8, 2004)

Key words: dynamic measurement, gas sensing behavior, influencing factors

The gas sensing behavior based on dynamic measurements of a single SnO₂ gas sensor was investigated by comparison with static measurements. The factors influencing nonlinear response such as modulation potential, duty ratio, heating waveform (rectangular, sinusoidal, saw-tooth, pulse, and others) were also studied. The temperature curves of the static and the dynamic measurements were investigated. Experimental data showed that temperature was the most important factor because changes in the frequency and the heating waveform could be the result of changes in temperature.

1. Introduction

Currently, although low-cost tin oxide gas sensors have previously been developed to achieve high selectivity for a particular chemical species, they also present some well-known problems (lack of selectivity, drift), which motivates active research in material science, different measurement strategies and signal processing algorithms. Different measurement strategies include sensors arrays, and static and dynamic measurements. Several studies have been focused on dynamic measurements including temperature transient or pulsed techniques and temperature modulation through oscillation of heater voltage, because it has been suggested that dynamic measurements using a single tin oxide sensor can provide more information than static measurements.^(1–21) In general, the information obtained from static measurements using chemical sensors is one-dimen-

*Corresponding author, e-mail address: xingjiu Huang@163.com

sional. For example, the change in the resistance of a semiconductor gas sensor (ΔR) or response and recovery time. However, these studies have always focused on identification of certain gases such as H_2S , CO , NO_2 , CO_2 , ethanol, methane, n-butane, ethane, propane, propylene and ammonia under a given constant heating waveform, frequency and operation temperature. There have been few detailed reports on the essential factors of dynamic measurements combined with different factors influencing dynamic responses.

In our previous work, we reported the rapid detection of pesticide residues using temperature modulation using only a single sensor rather than an array. We also reported that the amplitudes of the higher harmonics caused by FFT exhibited characteristic changes that depended not only on the chemical family of the pesticide gases but also on the concentration of pesticide gases as determined by the dynamic responses of the sensor.^(22,24)

In this paper, we report the advantages of dynamic measurements, and discuss the factors influencing nonlinear responses, such as modulation potential, duty ratio, heating waveform (rectangular, saw-tooth, pulse, sinusoidal), throughout the experimental trials. In addition, we also discuss the nature of these factors influencing nonlinear responses.

2. Experimental

A sol was prepared using a mixed ethanol solution of $SnCl_2$, $SbCl_3$, $CaCl_2$ and $SrCl_2$. The amounts of Sb, Ca and Sr were fixed to 2.5 mol% as M/Sn (M=Sb, Ca, Sr). As a binder, a given amount of commercial glass powder was added to the doped SnO_2 powder formed by calcinating the powder at $500^\circ C$ for 1/2 h in air. The screen print technique was used to prepare SnO_2 thick films on alumina ceramic substrates with a RuO_2 layer as a heating element on the back. The thick films were sintered at various temperatures for 1/2 h in air to obtain doped SnO_2 thick film gas sensors. These elements were aged at the working temperature until obtaining reproducible, steady-state resistances.

Butanone, acetone, ethanol, methanol, formaldehyde and cyclohexanone (analytical standards, provided by Sigma-Aldrich Laborchemikalien GmbH) were measured. The signal producing circuit boards were made by ECU Electronics Industrial Co., LTD (No.38 Research Institute of China Electronics & Technology Group Corp., China). The sensor resistance was monitored, acquired and stored in a PC for further analysis. Figure 1 shows the experimental setup. The measurement process was as follows: a given sample gas was injected into the testing chamber. Data acquisition started at 80 s before the diffusion of the injection gas reached equilibrium under stirring. The sampling rate was set at two points per second, and it took several minutes to complete measurements. The surface temperature of the sensing element was measured with an infrared thermometer (Keyence, IT2-01, Japan).

3. Results and Discussion

3.1 Static responses of SnO_2 -based gas sensors

The static responses of the SnO_2 sensor to 0.5 ppm butanone, acetone, ethanol, methanol and formaldehyde at an applied potential of 7 V are reported in Fig. 2. As shown in the figure, the resistance of the sensing element obviously changes upon exposure to the

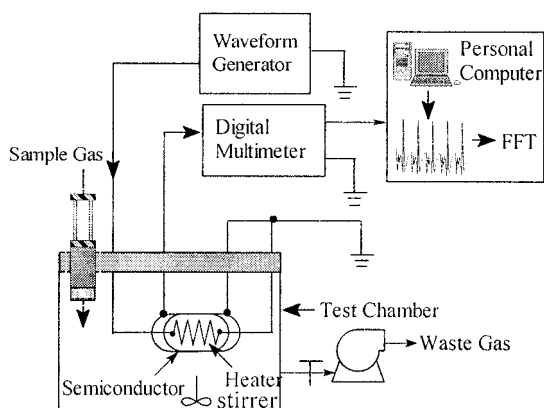


Fig. 1. Experimental setup.

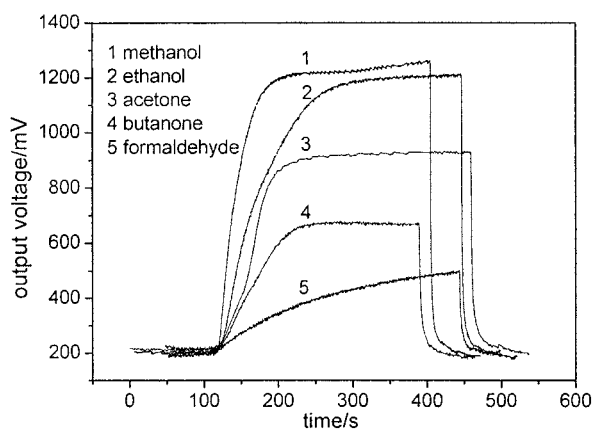


Fig. 2. Static responses to butanone, acetone, ethanol, methanol and formaldehyde. Experimental conditions: applied potential, 7 V; sample concentration, 0.5 ppm.

organic gas; meanwhile, the response time can be observed from the trend of the static curves. It is also necessary to point out, however, in addition to the changes in resistance and response time there is no other information about reaction processes, so it is difficult to analyze the mechanism by which the butanone, acetone, ethanol and methanol are detected. Except for the static response to formaldehyde, the responses are similar. In fact there are two functional groups: the carbonyl group and the hydroxyl group. We have no way to distinguish between carbonyl and hydroxyl groups because the sensor responses lack sufficiently different characteristics. During static measurements, only the resistance changes of the sensing element in the initial and final states are observed; no other information is obtained from other changes during the reaction processes.

3.2 Dynamic nonlinear responses of SnO_2 -based gas sensors

Figure 3 reports the dynamic nonlinear responses of a single SnO_2 gas sensor to 0.5 ppm ethanol, methanol, formaldehyde and cyclohexanone. Experimental conditions were as follows: applied potential, 7 V; duty ratio, 30 s/50 s; rectangular mode. Duty ratio is defined as $RA = t_h/(t_h+t_l)$, where t_h and t_l are the times of high level and low level, respectively.

First, as seen in Fig. 3, it is worth noting that there is sufficient information in the dynamic nonlinear responses to identify the sample gases easily by the different nonlinear responses. In the four selected species, there are three different functional groups: the hydroxyl group, the aldehyde group and a cyclic ketone; one can easily observe distinguishing features and connections among the samples by comparing their static responses. In the case of the dynamic responses to ethanol and methanol, because of their identical functional group, the curves have similar tendencies.

Second, it is widely accepted that oxygen in air can be chemisorbed and decomposed as O_2^- , O^- and O^{2-} . At a constant temperature, an equilibrium state exists at the surface of the SnO_2 sensing material: $\text{O}_2 \leftrightarrow \text{O}_2^-(\text{ad}) \leftrightarrow \text{O}^-(\text{ad}) \leftrightarrow \text{O}^{2-}(\text{ad})$. Semiconductor gas sensors monitor changes in the conductance during the interaction of a chemically sensitive

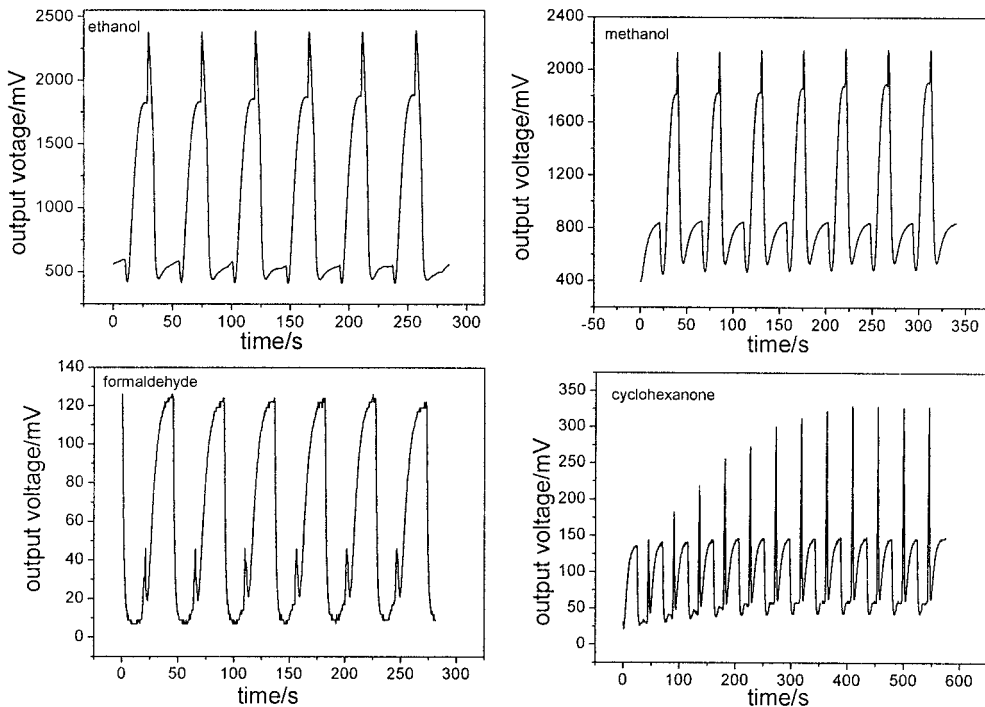


Fig. 3. Dynamic nonlinear responses to ethanol, methanol, formaldehyde and cyclohexanone. Experimental conditions: sample concentration, 0.5 ppm; applied potential, 7 V; duty ratio, 30 s/50 s; rectangular temperature mode.

material such as SnO_2 with molecules to be detected in the gas phase. The reaction steps involve low-temperature surface reactions and high-temperature bulk reactions between point defects in the SnO_2 crystal and oxygen (O_2) in the gas phase. The first step is adsorption followed by catalytic reactions at active sites (the latter involving intrinsic point defects, such as oxygen vacancies, and/or extrinsic point defects, such as segregated metal atoms) and similar reactions at grain boundaries or at three-phase boundaries (*e.g.*, at metallic contacts on surface metallic clusters). All these reactions involve adsorbed negatively charged molecular (O^{2-}) or atomic (O^-) oxygen species as well as hydroxyl groups (OH) at different surface sites.

During static measurements, adsorbed oxygen oxidizes sample gases on the surface, and the chemisorbed oxygen concentration decreases, inducing an increase in conductance. As seen from Fig. 3, gas identification in a rectangular temperature modulated mode is related to the different reaction kinetics of the interacting gases on the tin oxide surface. It is clear that, by temperature modulation, it is possible to provide surface oxygen species at constant temperatures which, under equilibrium conditions, do not exist. In this way, the reaction with the reducing and oxidizing gases is dramatically influenced, *e.g.*, at lower temperatures and at higher temperatures, the responses to sample gases exhibit their characteristic wave shapes due to reactions with different oxygen species. From these observations, we suggest that dynamic nonlinear responses are beneficial for analyzing the detection mechanism of the sample gases.

Third, the operating temperature during the dynamic processes is lower than that of the static processes. For example, the static operating temperature at an applied potential of 5 V reaches 346°C , whereas the dynamic temperature at an operating duty ratio of 30 s/50 s is in the range of $267\text{--}307^\circ\text{C}$; the experimental data is shown in Fig. 4. Therefore, we suggest that a modulated temperature operating mode not only enhances the selectivity of the gas sensor but also reduces its overall power consumption.

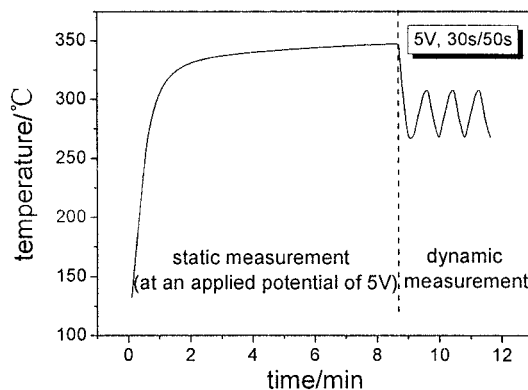


Fig. 4. The temperature curves at a constant duty ratio of 30 s/50 s. Controlling an applied potential of 5 V; rectangular modulation.

3.3 Effect of applied potential at duty ratio of 30 s/50 s

To optimize the selectivity of a temperature-modulated sensor, it is necessary to establish a relationship between a given potential and the sensor conductance in the presence of a specific gas. Figure 5 reports the effect of a given potential on the response of 0.5 ppm acetone at a constant duty ratio of 30 s/50 s in a rectangular mode. As seen in the figure, the different responses at different operating potential are easily observed. In this case the sensor exhibits enhanced selectivity to acetone as potential increases. It suggests that acetone can be identified by a relatively complete response at a potential of 7 V. Obviously, there are different surface reaction mechanisms for acetone and chemisorbed oxygen at different given operating potentials.

3.4 Effect of duty ratio at applied potential of 7 V

Figure 6 clearly shows the time-dependent shape change of the resistance of the sensor in the presence of butanone in air at different duty ratios obtained by controlling the applied potential of 7 V in a rectangular mode. As seen in the figure, one can easily observe the effects of turning the current on and off on the dynamic responses. In the left of the figure, the current being on evidently influences the lower half of the response; as the on-time lengthens (maintaining the electrical outage time in a thermal cycle), the response appears gradually. Inversely, the upper half of the response is obviously influenced by the off state; the longer the current is off, the more evident the upper half of the response. Therefore, the

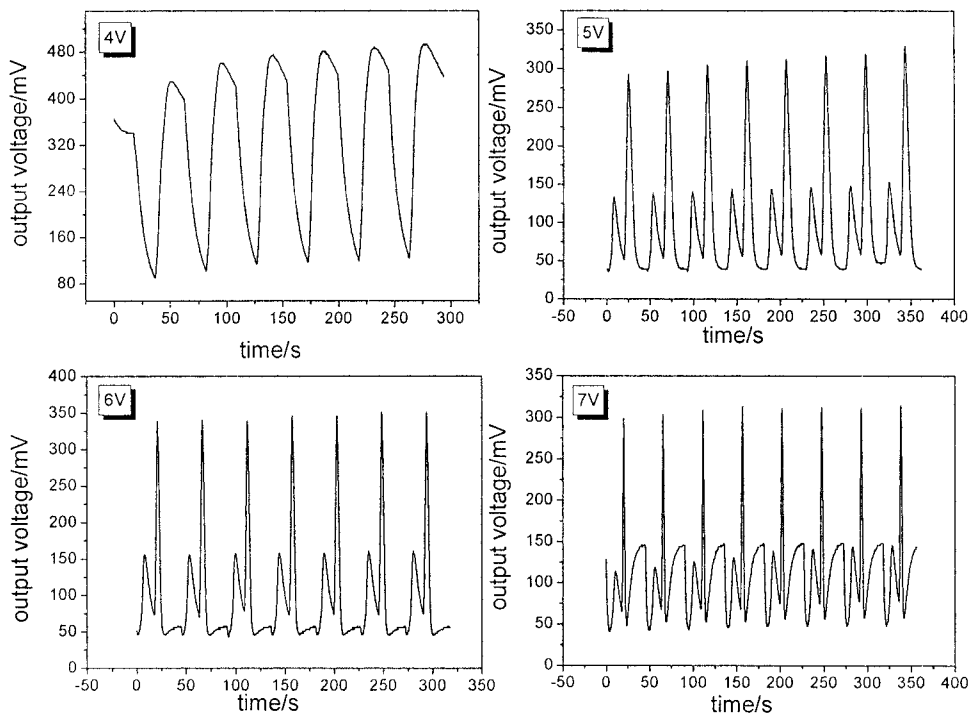


Fig. 5. Effect of applied potential on the responses to 0.5 ppm acetone at a duty ratio of 30 s/50 s in a rectangular mode.

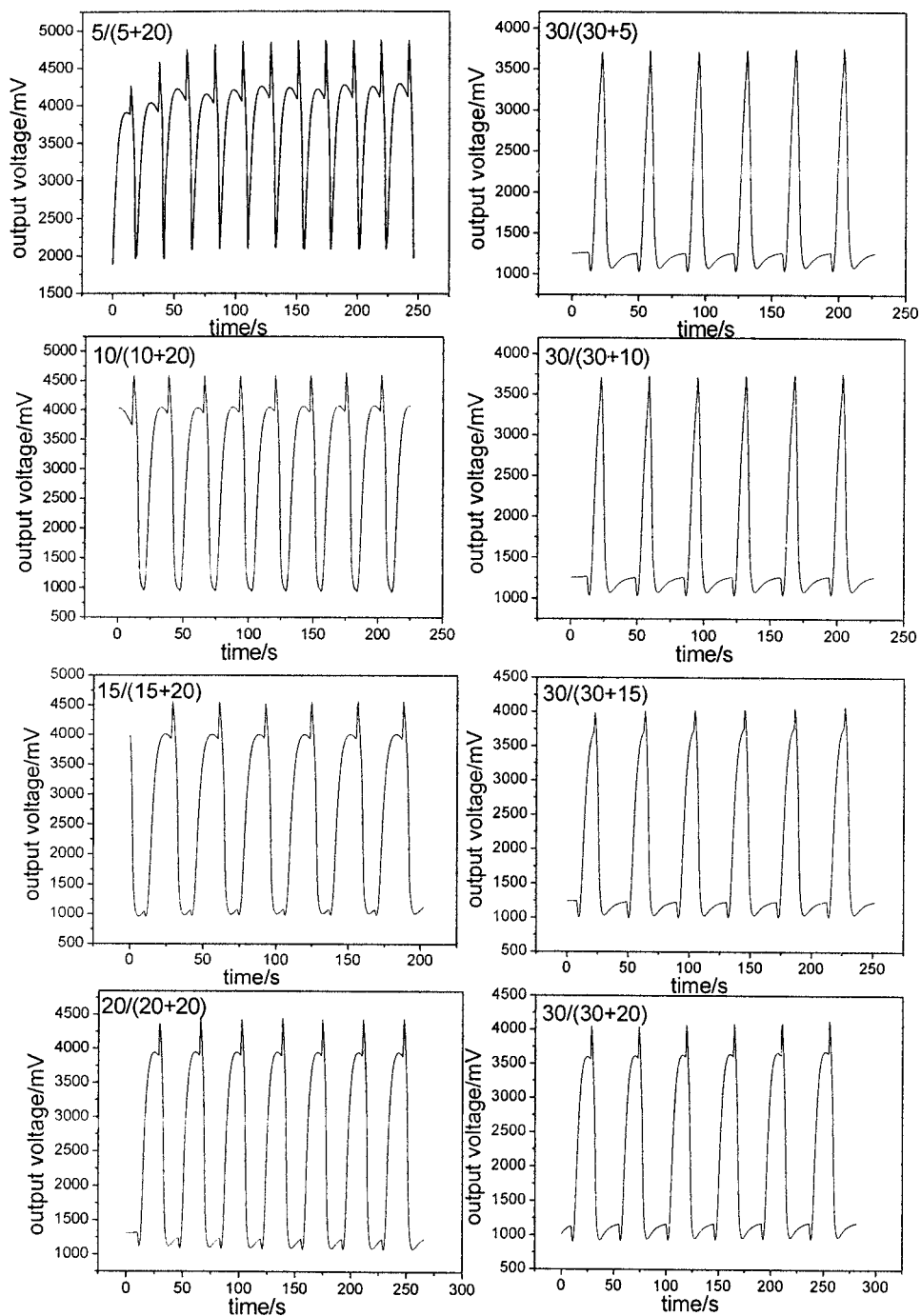


Fig. 6. Effect of duty ratio on the responses to ethanol at an applied potential of 7V in a rectangular mode.

duty ratio is beneficial to the investigation of the sensing mechanism, and it agrees with the analysis based on the dynamic nonlinear responses.

3.5 Effect of modulating waveform

To improve detection, the wave shape is modulated. The dynamic nonlinear responses of methanol are shown in Fig. 7 using different modulated waveforms. Although the object is the same, we can see that the nonlinear responses are different for each waveform. These experimental data were in agreement with those reported by Ortega *et al.* Ortega *et al.* have reported that CO and CH₄ can be detected using pulse and triangular heating waveforms.⁽¹⁹⁾ According to the above analysis, we know that a change in heating shape waveform influences the sensing behavior of a sample gas due to the changes in the surface temperature of the sensing element.

3.6 Changes of surface temperature under different applied potentials

To investigate the nature of the factors influencing sensor response, taking applied potential as an example, the relative intensities of surface temperature under different applied potentials are reported in Fig. 8. It is found that the surface temperature changes are similar to each other under the squared modulation duty ratio and different applied

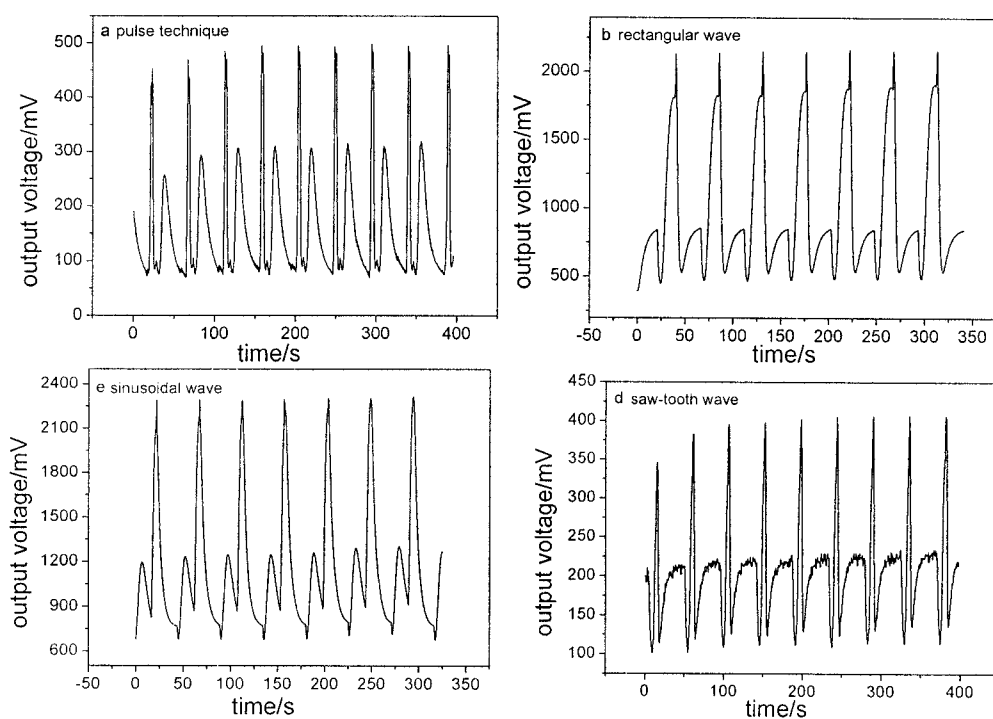


Fig. 7. Effect of modulation waveform on the dynamic response of methanol. Experimental conditions: applied potential 7 V, modulation frequency 20 mHz.

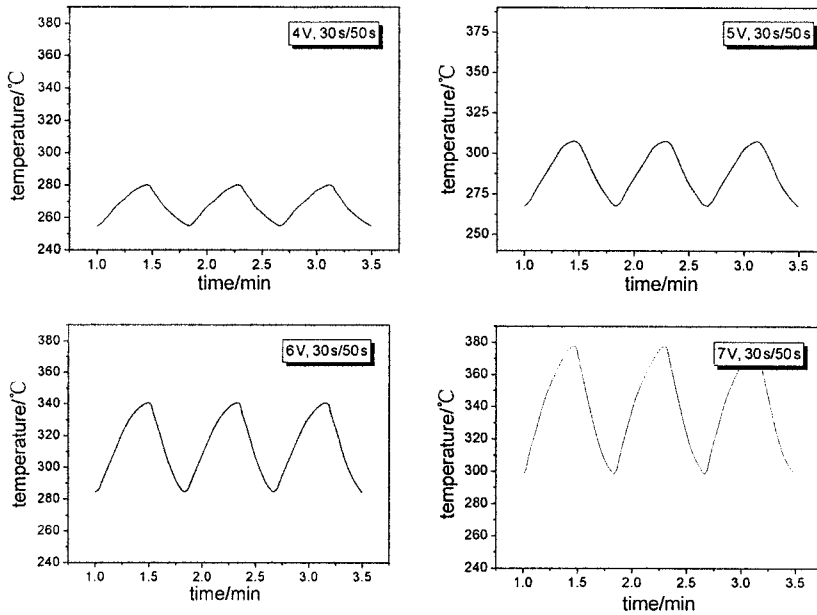


Fig. 8. The temperature curves under different applied potentials; rectangular modulation. Their corresponding dynamic responses are shown in Fig. 5.

potentials. However, it is worth noting that, first, the maximum and minimum temperatures are different under various operation voltages, and second, the surface temperature variation range differs with the different applied potentials; the temperature range reaches maximum at an applied potential of 7 V. This demonstrates that the temperature range has a significant effect on the dynamic response. Third, the higher the applied potential, the less obvious the “hysteresis effect” of temperature variation on the sensor surface. The “hysteresis effect” is that the sensor surface temperature does not vary in-step with the time variation of duty ratios. Because of the “hysteresis effect” the responses are unstable at applied potentials of 4 V and 5 V (Fig. 5). It is necessary to point out that, although the temperature curves are similar to each other under different conditions, the temperature gradients $\partial T / \partial \tau$ are obviously different, where T and τ are the surface temperature of the sensor and the corresponding time, respectively. These data show that the strenuous extents of surface temperature are different from each other with changes in time. Different temperatures result in different surface resistances.

4. Conclusions

This study of dynamic and static measurements has allowed us to demonstrate the advantage of the former type of measurements to maximize the information extracted from a single gas sensor. Experimental tests show that dynamic measurement is beneficial to facilitate the most significant output signal to separate the sample gases. Meanwhile, a

variety of influential factors such as modulation potential, duty ratio, heating waveform (rectangular, saw-tooth, pulse, sinusoidal) were investigated. The characteristic optimum oxidation potential of acetone was 7 V at a duty ratio of 30 s/50 s. At a constant duty ratio (30 s/50 s), the temperature contrast reached a maximum which was beneficial for detecting butanone. Experimental data also show that different waveforms improve the detection if the separation of certain gases is not clear. Finally, all data show that temperature is the most important influential factor.

Acknowledgement

This work was financially supported by the National Natural Science Foundation of China (project 60274061) and the Anhui Province Natural Science Foundation (project 01041404); both are gratefully acknowledged.

References

- 1 Y. Hiranaka, T. Abe and H. Murata: *Sensors and Actuators B* **9** (1992) 177.
- 2 T. Amamoto, T. Yamaguchi, Y. Matsuura and Y. Kajiyama: *Sensors and Actuators B* **13** (1993) 587.
- 3 J. Kelleter, C.-D. Kohi and H. Petig: US Pat. 5668304, September **16** (1997).
- 4 R. Aigner, F. Auerbach, P. Huber, R. Muller and G. Scheller: *Sensors and Actuators B* **18** (1994) 143.
- 5 S. Nakata and H. Nakamura: *Sensors and Actuators B* **8** (1992) 187.
- 6 S. Nakata, Y. Kaneda, H. Nakamura and K. Yoshikawa: *Chem. Lett.* (1991) 1505.
- 7 P. Romppainen, V. Lantto and S. Leppavuori: *Sensors and Actuators B* **1** (1990) 73.
- 8 V. Lantto and P. Romppainen: *J. Electrochem. Soc.* **135** (1988) 2550.
- 9 Y. Kato, K. Yoshikawa and M. Kitora: *Sensors and Actuators B* **40** (1997) 33.
- 10 N.-J. Choi, Ch.-H. Shim, K.-D. Song, K.-S. Lee, J.-S. Huh and K.-D. Lee: *Sensors and Actuators B* **86** (2002) 251.
- 11 M. Roth, R. Hartinger, R. Faul and H.-E. Endres: *Sensors and Actuators B* **35** (1996) 358.
- 12 A. P. Lee and B. J. Reedy: *Sensors and Actuators B* **60** (1999) 35.
- 13 S. Nakata, E. Ozaki and N. Ojima: *Analytica Chimica Acta.* **361** (1998) 93.
- 14 S. Nakata, M. Nakasuji, N. Ojima and M. Kitora: *Applied Surface Science* **135** (1998) 285.
- 15 A. Fort, M. Gregorkiewitz, N. Machetti, S. Rocchi, B. Serrano, L. Tondi, N. Ulivieri, V. Vignoli, G. Faglia and E. Comini: *Thin Solid Films* **418** (2002) 2.
- 16 R. Aigner, M. Dietl, R. Katterloher and V. Klee: *Sensors and Actuators B* **33** (1996) 151.
- 17 A. Heilig, N. Barsan, U. Weimar, M. Schweizer-Bergerich, J. W. Gardner and W. Göpel: *Sensors and Actuators B* **43** (1997) 45.
- 18 R. E. Cavicchi, J. S. Suehle, K. G. Kreider, M. Gaitan and P. Chaparala: *Sensors and Actuators B* **33** (1996) 142.
- 19 A. Ortega, S. Marco, A. Perera, T. Sundic, A. Pardo and J. Samitier: *Sensors and Actuators B* **78** (2001) 32.
- 20 R. Ionescu and E. Llobet: *Sensors and Actuators B* **81** (2002) 289.
- 21 S. Nakata and N. Ojima: *Sensors and Actuators B* **56** (1999) 79.
- 22 X. -J. Huang, J. -H. Liu, D. -L. Shao, Z. -X. Pi and Z. -L. Yu: *Sensors and Actuators B* **96** (2003) 630.
- 23 X. -J. Huang, L. -Ch. Wang, Y. -F. Sun, F. -L. Meng and J. -H. Liu: *Sensors and Actuators B* **99** (2004) 330.
- 24 X. -J. Huang, J. -H. Liu, Z. -X. Pi and Z. -L. Yu: *Talanta* **64** (2004) 538.